

# Investigations of Water Structure at the Solid/Liquid Interface in the Presence of Supported Lipid Bilayers by Vibrational Sum Frequency Spectroscopy

Joonyeong Kim, Gibum Kim, and Paul S. Cremer\*

Department of Chemistry, Texas A&M University, P.O. Box 30012,  
College Station, Texas 77842-3012

Received December 11, 2000. In Final Form: July 31, 2001

The structure of water was investigated at the quartz/water interface in the presence of supported lipid bilayers (SLBs) by the use of infrared–visible sum frequency spectroscopy. By varying the pH of the bulk solution and the charge on the SLB, changes in both ice-like and water-like peaks were observed in the OH stretch region with respect to the plain quartz/water interface. The oscillator strengths were most affected by applying charged SLBs, rather than bilayers that did not contain a net charge. Time-dependent studies of the ice-like peak intensity at pH 5.6 during the fusion of lipid vesicles to the bare quartz surfaces revealed that the formation rate of a negatively charged SLB was much slower than that of positively charged and neutral SLBs.

## Introduction

Solid supported lipid bilayers (SLBs) have been the subject of increasing interest over the past decade due to their ability to mimic many properties of biological membranes including two-dimensional fluidity (Figure 1).<sup>1–6</sup> Lateral diffusion of bilayer components is crucial to the behavior of cell surfaces because multivalent interactions between membrane bound ligands and aqueous receptors require substantial rearrangements to take place in the membrane in order to initiate signaling events and optimize binding.<sup>7–10</sup>

Upon initial examination, the fluidity of lipid bilayers supported on glass substrates may appear surprising. Indeed, phospholipid molecules in the lower leaflet of the membrane might be expected to interact too strongly with the underlying support to maintain mobility comparable to that of free bilayers and cell membranes. However, a large body of experimental evidence suggests that a thin layer of water resides between the lower leaflet of the bilayer and the underlying substrate.<sup>11–14</sup> It is generally accepted that this two-dimensionally confined water layer, which has been estimated to be approximately 0.5–1.5 nm in thickness, acts as a lubricant to allow lipid

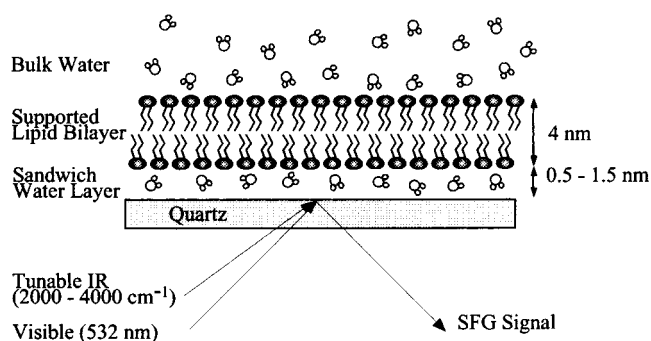


**Figure 1.** A planar supported phospholipid bilayer on a quartz substrate. Two input laser beams, visible and tunable infrared, are focused onto the interface to produce SFG signal.

bilayers to facily move in the plane of the surface (Figure 1). Unfortunately, little chemical and structural information on this highly confined water layer is available.

Obtaining detailed structural information on water confined at interfaces represents a substantial experimental challenge. This stems from the paucity of spectroscopic characterization techniques available for probing interfacial water in the presence of an overwhelming bulk contribution. In the past few years, infrared–visible sum frequency generation (SFG), a surface specific vibrational spectroscopy, has been emerging as a viable technique for obtaining information about a number of aqueous interfaces.<sup>15–26</sup> In particular, SFG data have helped

\* To whom correspondence should be addressed: Tel 979-862-1200, Fax 979-845-7561, e-mail cremer@mail.chem.tamu.edu.

(1) Tamm, L. K.; McConnell, H. M. *Biophys. J.* **1985**, *47*, 105.  
(2) Sackmann, E. *Science* **1996**, *271*, 43.  
(3) Tampe, R.; Dietrich, C.; Gritsch, S.; Elender, G.; Schmitt, L. *Nanofabrication and Biosystems: Integrating Materials Science, Engineering, and Biology*; Cambridge University Press: New York, 1996.  
(4) Cremer, P. S.; Boxer, S. G. *J. Phys. Chem. B* **1999**, *103*, 2554.  
(5) Gennis, R. B. *Biomembranes: Molecular Structure and Function*; Springer-Verlag: New York, 1989.  
(6) Groves, J. T.; Ulman, N.; Boxer, S. G. *Science* **1997**, *275*, 651.  
(7) Mammen, M.; Choi, S. K.; Whitesides, G. M. *Angew. Chem., Int. Ed.* **1998**, *37*, 2754.  
(8) Mann, D. A.; Kanai, M.; Maly, J.; Kiessling, L. L. *J. Am. Chem. Soc.* **1998**, *120*, 10575.  
(9) Burke, S. D.; Zhao, Q.; Schuster, M. C.; Kiessling, L. L. *J. Am. Chem. Soc.* **2000**, *122*, 4518.  
(10) Kiessling, L. L.; Pohl, N. L. *Chem. Biol.* **1996**, *3*, 71.  
(11) Bayerl, T. M.; Bloom, M. *Biophys. J.* **1990**, *58*, 357.  
(12) Johnson, S. J.; Bayerl, T. M.; McDermott, D. C.; Adam, G. W.; Rennie, A. R.; Thomas, R. K.; Sackmann, E. *Biophys. J.* **1991**, *59*, 289.  
(13) Koenig, B. W.; Krueger, S.; Orts, W. J.; Majkrzak, C. F.; Berk, N. F.; Silverton, J. V.; Gawrisch, K. *Langmuir* **1996**, *12*, 1343.  
(14) Mou, J. X.; Shao, Z. F. *Biochemistry* **1994**, *33*, 4439.

(15) Kim, J.; Cremer, P. *J. Am. Chem. Soc.* **2000**, *122*, 12371.  
(16) Du, Q.; Superfine, R.; Freysz, E.; Shen, Y. R. *Phys. Rev. Lett.* **1993**, *70*, 2313.  
(17) Du, Q.; Freysz, E.; Shen, Y. R. *Science* **1994**, *264*, 826.  
(18) Du, Q.; Freysz, E.; Shen, Y. R. *Phys. Rev. Lett.* **1994**, *72*, 238.  
(19) Miranda, P. B.; Xu, L.; Shen, Y. R.; Salmeron, M. *Phys. Rev. Lett.* **1998**, *81*, 5876.  
(20) Gragson, D. E.; Richmond, G. L. *J. Chem. Phys.* **1997**, *107*, 9687.  
(21) Gragson, D. E.; McCarty, B. M.; Richmond, G. L. *J. Am. Chem. Soc.* **1997**, *119*, 6144.  
(22) Gragson, D. E.; Richmond, G. L. *J. Phys. Chem. B* **1998**, *102*, 3847.  
(23) Gragson, D. E.; Richmond, G. L. *J. Am. Chem. Soc.* **1998**, *120*, 366.  
(24) Schnitzer, C.; Baldelli, S.; Shultz, M. J. *J. Phys. Chem. B* **2000**, *104*, 585.

elucidate the structure of water at the quartz/water interface.<sup>15,18</sup> These results reveal that interfacial water molecules are highly ordered in comparison to bulk water, and that their particular structure depends on the prevailing pH.

The SFG technique has been described in detail elsewhere.<sup>27–29</sup> Briefly, SFG is a second-order nonlinear optical process in which two input beams with frequencies  $\omega_{\text{ir}}$  and  $\omega_{\text{vis}}$  overlap in a medium to generate an output at the sum frequency,  $\omega_{\text{sfg}}$ . As a second-order process, SFG is forbidden in media that possess inversion symmetry but allowed at surfaces and interfaces where inversion symmetry is necessarily broken. This technique, therefore, can be employed as an interface specific probe for systems with bulk inversion symmetry. The intensity of the SFG signal,  $I_{\text{sfg}}$ , is proportional to the square of the surface nonlinear susceptibility,  $\chi_s^{(2)}$ :

$$I_{\text{sfg}} \approx |P_{\text{sfg}}|^2 \approx |\chi_s^{(2)}|^2 I_{\text{vis}} I_{\text{ir}} = |\chi_{\text{NR}}^{(2)} e^{i\delta\nu} + \sum |\chi_{\text{Rv}}^{(2)}|^2 I_{\text{vis}} I_{\text{ir}} \quad (1)$$

$$\chi_{\text{Rv}}^{(2)} \approx A_v / (\omega_v - \omega_{\text{ir}} - i\Gamma_v) \quad (2)$$

where  $\chi_{\text{NR}}^{(2)}$  and  $\chi_{\text{Rv}}^{(2)}$  denote the nonresonant and resonant contributions, respectively. The term  $e^{i\delta\nu}$  is a phase factor, and  $A_v$ ,  $\omega_v$ , and  $\Gamma_v$  are the oscillator strength, resonant frequency, and damping constant of the  $v$ th resonant mode, respectively.

Here we report the results of SFG investigations at the quartz/water interface in the presence of negatively charged, positively charged, and net neutral planar lipid bilayers. The SFG results reveal substantial changes in interfacial water structure upon vesicle fusion to the surface.

## Experimental Section

**A. Laser System.** SFG spectra were obtained with a passive-active mode-locked Nd:YAG laser (PY61c, Continuum, Santa Clara, CA) equipped with a negative feedback loop in the oscillator cavity to provide enhanced shot to shot stability. The 1064 nm light generated had a pulse width of 21 ps, and the laser was operated at a 20 Hz repetition rate. Radiation was sent to an optical parametric generator/amplifier (OPG/OPA) stage (Laser Vision, Bellevue, WA) where tunable infrared radiation was produced in addition to frequency-doubled radiation at 532 nm. The OPG/OPA consisted of two parts. The first was an angle tuned potassium titanyl phosphate (KTP) stage pumped with 532 nm light to generate near-infrared radiation between 1.35 and 1.85  $\mu\text{m}$ . This output was then mixed with the 1064 nm fundamental in an angle tunable potassium titanyl arsenate (KTA) stage to produce a tunable infrared beam from 2000 to 4000  $\text{cm}^{-1}$  (7  $\text{cm}^{-1}$  fwhm). The intensity of the radiation was approximately 500  $\mu\text{J}/\text{pulse}$  near 3500  $\text{cm}^{-1}$ . The tunable IR beam was combined with 532 nm radiation at the interface at incident angles of 51° and 42° with respect to the surface normal. The power of the 532 nm beam, which was generated in an initial KTP stage, was 1 mJ/pulse at the sample. The SFG signal generated from the sample was detected by a photomultiplier tube, sent to a gated integrator, and stored digitally. All spectra presented in this paper were collected with the  $S_{\text{sfg}}$ ,  $S_{\text{vis}}$ , and  $P_{\text{ir}}$  polarization combination. For each scan, data were collected in 6  $\text{cm}^{-1}$  increments in the 2800–3600  $\text{cm}^{-1}$  range and normalized to a piece of Y-cut crystalline quartz.

(25) Baldelli, S.; Schnitzer, C.; Shultz, M. J. *J. Phys. Chem. B* **1997**, *101*, 10435.

(26) Baldelli, S.; Schnitzer, C.; Shultz, M. J. *J. Phys. Chem. B* **1997**, *101*, 4607.

(27) Shen, Y. R. *Nature* **1989**, *337*, 519.

(28) Shen, Y. R. *Surf. Sci.* **1994**, *299/300*, 551.

(29) Guyot-Sionnest, P.; Hunt, J. H.; Shen, Y. R. *Phys. Rev. Lett.* **1988**, *59*, 1597.

**B. Sample Preparation.** The purified water used for the preparation of buffer solutions and for the cleaning of the experimental apparatus was produced from a NANOpure Ultrapure Water System (Barnstead, Dubuque, IA) with a minimum resistivity of 18  $\text{M}\Omega\cdot\text{cm}$ . Twelve aqueous solutions with pH values of 1.5, 3.8, 5.6, 8.0, 10.0, and 12.3 and total electrolyte concentrations (concentrations of negatively and positively charged ions divided by 2) of 32 and 150 mM were prepared with purified water by adding appropriate amounts of 0.5 M HCl for solutions with pH 1.5, 0.5 M NaOH for solutions with pH 10.0 and 12.3, and sodium phosphate/phosphoric acid for solutions with pH values of 3.8, 5.6, and 8.0. NaCl was used to increase the total electrolyte concentration of the solutions to the desired value.

The infrared-grade fused quartz windows used in these studies (o.d. 1 in. and thickness 1/16 in.) were purchased from Quartz Plus Inc. (Brookline, NH) and cleaned in hot chromic acid solution for at least 3 h, rinsed extensively with purified water, and baked overnight in a kiln at 400 °C before use. Atomic force microscopy (AFM) images showed that these windows were nearly flat with a root-mean-square roughness of 0.45 nm over a 3  $\mu\text{m} \times 5 \mu\text{m}$  area.

Egg phosphatidylcholine (egg PC), dimethyldioctadecylammonium bromide (DDAB), and 1,2-dilauroyl-*sn*-glycero-3-[phospho-1-serine] sodium salt (DLPS) were purchased from Avanti Polar Lipid Inc. (Alabaster, AL) and used without further purification. Neutral (100% egg PC), positively charged (90 mol % egg PC, 10 mol % DDAB), and negatively charged (90 mol % egg PC with 10 mol % DLPS) small unilamellar vesicles (SUVs) were prepared following standard procedures.<sup>4,30</sup> Briefly, lipid mixtures in chloroform were dried under a flowing nitrogen stream and reconstituted in sodium phosphate buffer solution (pH 8.0, total electrolyte concentration of 32 mM). The suspension was then probe sonicated to clarity over an ice bath in a nitrogen atmosphere and centrifuged at 38 000 rpm (94 500g) for 30 min. The supernatant was then centrifuged again at 52 000 rpm (176 900g) for 3 h at 4 °C. The final supernatant obtained was used in all studies and had a concentration of approximately 1.7 mg/mL. Thin-layer chromatography and dynamic light scattering measurements (PD2000DLS, Precision Detectors Inc.) revealed that this procedure did not lead to lipid hydrolysis or oxidation.

**C. Flow Cell Design for SFG Experiments.** SFG measurements were carried out using a homemade flow cell (volume, ca. 2.0 mL) which consisted of a machined Teflon body fitted with a fused quartz plate. The sides of the cell had an inlet and an outlet port to which Tygon tubing (i.d. 0.06 in.) was attached for flowing liquid. The incoming laser beams were focused concentrically on the bottom face of the fitted quartz plate where supported lipid bilayers were formed. The creation of SLBs was achieved by the vesicle fusion method at pH 5.6 and a total electrolyte concentration of 32 mM except for the negatively charged bilayers, which were formed at pH 3.8. About 5.0 mL of each SUV solution was introduced into the flow cell, allowed to incubate for at least 30 min to form the supported bilayer, and finally washed out with pure buffer solution at pH 5.6 (pH 3.8 for negatively charged SLBs) and a total electrolyte concentration of 32 mM. To change the pH of the bulk solution in the flow cell in the presence of SLBs, stock solution at the desired pH was flowed until the pH value at the outlet port varied by less than  $\pm 0.1$  pH unit compared to the target pH. As the charged SLBs contain lipid components which differed from egg PC in both headgroup and alkyl chain length, the formation and stability of the SLBs were carefully investigated by fluorescence microscopy and differential scanning calorimetry (Shimadzu DSC-50). SLBs were formed using SUV solutions containing 0.5 mol % of Texas red labeled 1,2-dihexadecanoyl-*sn*-glycero-3-phosphoethanolamine, triethylammonium salt (Molecular Probes, Portland, OR), and fluorescence microscopy revealed the formation of uniform fluid supported bilayers over the entire pH range investigated down to at least the diffraction limit. In agreement with the fluorescence measurements, differential scanning calorimetry data of lipid vesicles without fluorescent probes confirmed that all phase transitions took place well below room

(30) Barenholz, Y.; Gibbes, D.; Litman, B.; Goll, J.; Thomson, T.; Carlson, F. *Biochemistry* **1977**, *16*, 2806.

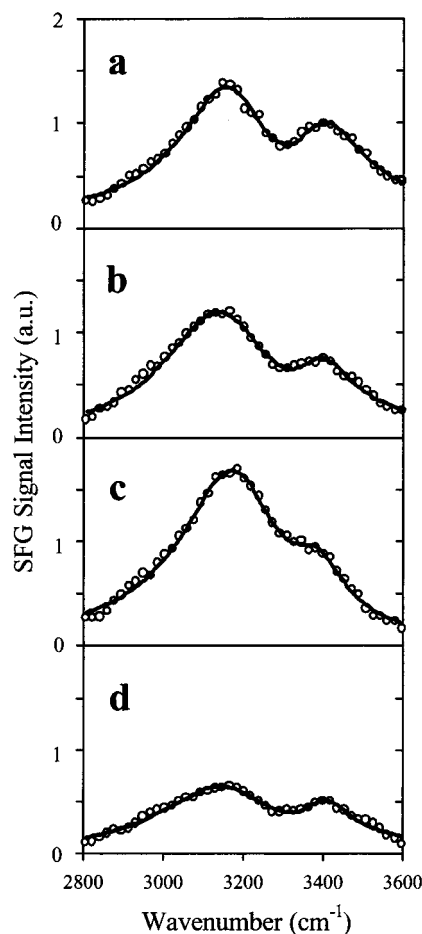


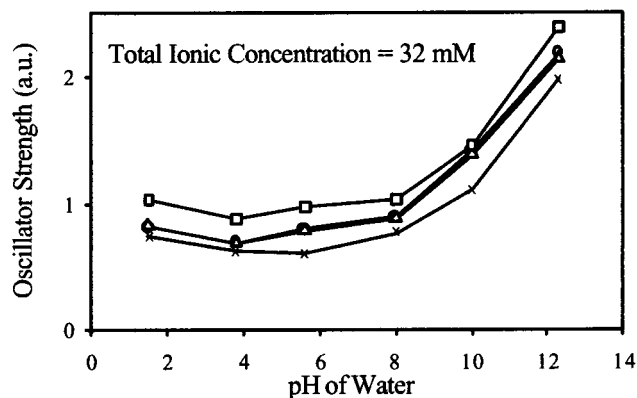
**Figure 2.** SFG spectra in the OH stretch region at the quartz/water interface at pH 5.6 and a total electrolyte concentration of 32 mM (a) without a lipid bilayer, (b) with a neutral SLB, (c) with a positive SLB, and (d) with a negative SLB. Open circles denote collected data. The solid lines are fits to the data using a Voigt profile.

temperature. Matrix-assisted laser desorption/ionization (MALDI) mass spectrometry showed that the chemical composition of the supported lipid bilayers remained unchanged from the SUV solutions from which they were formed.<sup>31</sup> SFG measurements at each set of pH and electrolyte values were repeated at least three times. All SFG measurements were carried out at 23 °C.

## Results

**A. pH Effects.** SFG spectra of the quartz/water/bilayer interface were obtained from pH 1.5 to 12.3 in the OH stretch range at a total electrolyte concentration of 32 mM. Representative data at pH 5.6 are shown in Figure 2, and the rest of these spectra are provided in the Supporting Information. Figure 2a presents data for the bare quartz/water interface and agrees with previous results.<sup>18</sup> Two major features are observed, one located at 3200  $\text{cm}^{-1}$  and the other 3400  $\text{cm}^{-1}$ . The first one is assigned to the coupled OH symmetric stretch mode from tetrahedrally coordinated water molecules at the interface. As ice exhibits strong intensity at 3200  $\text{cm}^{-1}$  in the vibrational spectrum, it is believed that this peak indicates the presence of “ice-like” structure.<sup>32,33</sup> The assignment of the feature near 3400  $\text{cm}^{-1}$  is somewhat less certain. The first possibility is an OH symmetric stretch from asymmetrically hydrogen-bonded water.<sup>32</sup> The second possibility is that the peak comes from water molecules with bifurcated hydrogen bonds.<sup>34</sup> Either assignment is indicative of water molecules with more disordered hydrogen bonding or a “water-like” molecular structure.

a. Ice-like Oscillator Strength at 3200  $\text{cm}^{-1}$



b. Water-like Oscillator Strength at 3400  $\text{cm}^{-1}$

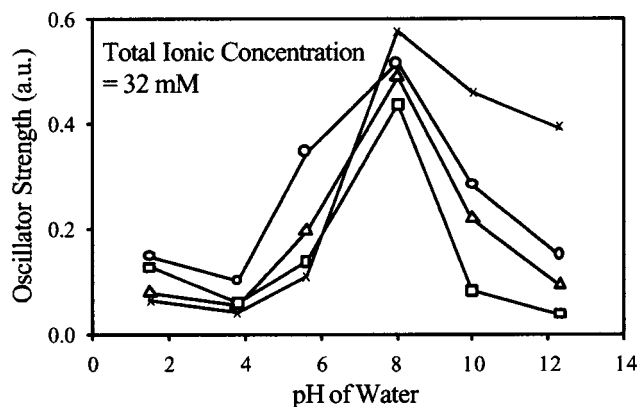


**Figure 3.** Fitted oscillator strengths of (a) the ice-like and (b) the water-like peaks from SFG spectra at pH 1.5, 3.8, 5.6, 8.0, 10.0, and 12.3 with a total electrolyte concentration of 32 mM. The data denote the bare quartz/water interface ( $\circ$ ) as well as surfaces coated with neutral SLBs ( $\triangle$ ), positively charged SLBs ( $\square$ ), and negatively charged SLBs ( $\times$ ). The error bars on all of these measurements are as small or smaller than the symbols employed in the plots.

Figure 2b shows SFG spectra of a quartz/water interface under the same conditions as in Figure 2a, but in the presence of a neutral egg PC bilayer. This spectrum bears a general resemblance to that shown in Figure 2a, although the 3400  $\text{cm}^{-1}$  peak is slightly smaller. The SFG spectra of positively (Figure 2c) and negatively (Figure 2d) charged SLBs show more significant changes with respect to the bare quartz/water interface.

To evaluate the data in a quantitative fashion, the values of the oscillator strengths ( $A_v$  in eq 2) from the 3200  $\text{cm}^{-1}$  mode are plotted as a function of pH in Figure 3a. As can be seen from the data, the oscillator strength associated with ice-like structure is especially strong at higher pH where a substantial electric field emanates from deprotonated surface silanol groups on the quartz substrate.<sup>36,37</sup> The interface coated with a positively charged bilayer ( $\square$ ) gives rise to the largest oscillator strength values over the entire pH range, while the surface coated with the negatively charged bilayer ( $\times$ ) gives rise to the weakest. The largest differences in oscillator strength (ca. 60%) occur at pH 5.6. Finally, the strength of the ice-like mode from the surface covered with the neutral egg PC bilayer ( $\triangle$ ) is very similar to the bare quartz surface ( $\circ$ ).

The oscillator strengths of the water-like peaks at 3400  $\text{cm}^{-1}$  are presented in Figure 3b. The highest values were seen at pH 8.0 for all four cases, and they attenuate at

both higher and lower pH. The negatively charged membrane ( $\times$ ) displays the most interesting behavior. At high pH (8.0, 10.0, and 12.3), the strength of the water-like peak from this system is greater than for all other conditions. However, at low pH (5.6, 3.8, and 1.5), it falls dramatically to yield the weakest water-like oscillator strength. It should be noted that the carboxylic acid moiety on DLPS becomes protonated near pH 6.0 and renders these bilayers neutral as the pH of the solution is lowered.<sup>5,38</sup> An important trend for most SLBs is the tendency of the bilayer to depress the water-like oscillator strength in comparison to the bare liquid/solid interface. This is especially evident at pH 5.6 where the water-like value from the bare surface ( $\circ$ ) is clearly much larger than for any of the bilayer-coated interfaces shown in Figure 3b. Indeed, with the exception of high pH conditions (12.3, 10.0, and 8.0) for membranes containing DLPS, the bare surface gives rise to the strongest water-like oscillator strengths under all conditions tested.

**B. Effects of Total Electrolyte Concentration.** All experiments performed above were repeated at a total electrolyte concentration of 150 mM. The figures corresponding to these data are provided in the Supporting Information. Figure 4 shows fitted results of the ice-like and water-like oscillator strengths at each pH analogous to Figure 3. The strengths of the ice-like peaks (Figure 4a) were reduced compared to the low electrolyte concentration case at pH 8.0, 10.0, and 12.3. At lower pH (5.6, 3.8, and 1.5) the oscillator strengths were nearly comparable. The water-like peaks (Figure 4b) also showed a general reduction in oscillator strength for higher electrolyte concentration. Again, surfaces coated with negatively charged SLBs gave rise to the strongest water-like strengths at high pH but the weakest strengths at low pH.

**C. Time-Dependent Effects.** In a final set of experiments, the SFG signal intensity ( $I_{\text{SFG}}$  in eq 1) was monitored at  $3200\text{ cm}^{-1}$  (ice-like peak) as a function of time during the flow of SUV solutions at pH 5.6 and a total electrolyte concentration of 32 mM. The results are shown in Figure 5. In each case, the SUV solution (1.7 mg/mL) was flowed beginning at  $t = 500\text{ s}$ . Accordingly, signal intensity between  $t = 0$  and 500 s represents the SFG signal from the bare quartz/water interface. The overall intensity was slightly reduced upon the formation of a neutral SLB (Figure 5a)<sup>35</sup> but enhanced by the formation of a positively charged SLB (Figure 5b). In both cases, signal changes were completed within  $\sim 300\text{ s}$  after the introduction of the vesicles. By contrast, relatively greater signal reduction was observed over  $\sim 800\text{ s}$  when SUVs with net negative charges were flowed (Figure 5c).

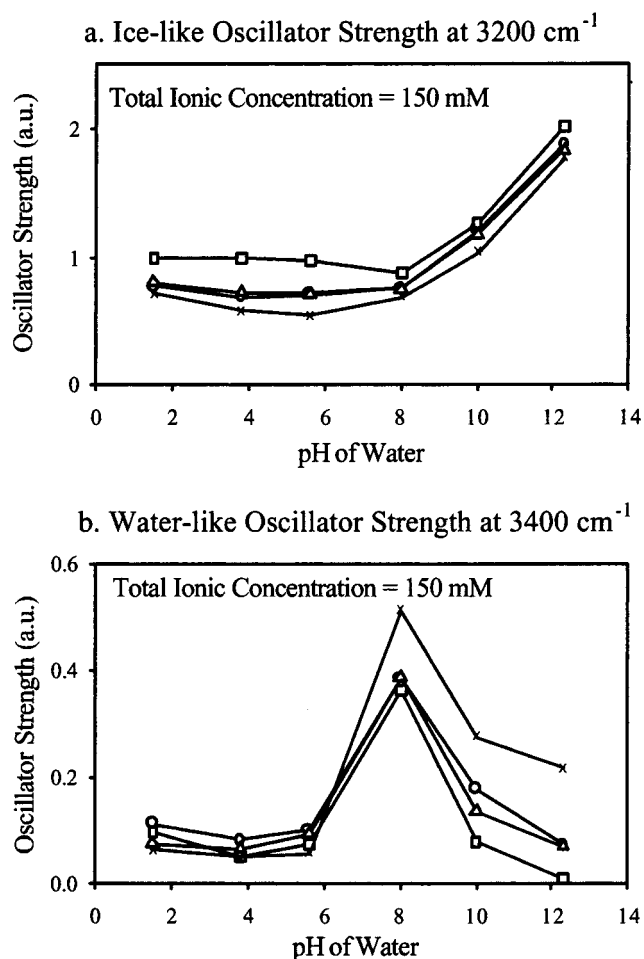


**Figure 4.** Fitted oscillator strengths of (a) the ice-like and (b) the water-like peaks from SFG spectra of the same conditions in Figure 3, but at a total electrolyte concentration of 150 mM. The data denote the bare quartz/water interface ( $\circ$ ) as well as surfaces coated with neutral SLBs ( $\Delta$ ), positively charged SLBs ( $\square$ ), and negatively charged SLBs ( $\times$ ). The error bars on all of these measurements are as small or smaller than the symbols employed in the plots.

## Discussion

The reordering of water molecules at the quartz/water interface upon bilayer formation depends intimately upon the specific conditions. At least two sources of interfacial signal from three interfaces (quartz/water, water/lower bilayer leaflet, and upper bilayer leaflet/bulk water) need to be considered (Figure 1). The first is the thin film of confined water between the SLB and the quartz surface.<sup>11–14</sup> This thin film will be referred to as “sandwich” water and will be the major focus of this discussion. The second contribution to the signal arises from interfacial water that is present at the boundary between the upper bilayer leaflet and the bulk aqueous solution.

**A. Bare Quartz/Water Interface.** The surface of clean quartz contains titratable silanol groups (ca.  $5\text{ Si-OH/nm}^2$ )<sup>18,36</sup> that can be deprotonated as the pH value of the bulk aqueous solution is raised. At high pH (12.3, 10.0, and 8.0), a considerable number of silanol groups on the quartz surface are ionized, which produces a correspondingly high surface charge density (ca.  $0.8\text{ C/m}^2$  at pH 12.3,  $0.5\text{ C/m}^2$  at pH 10.0, and  $0.2\text{ C/m}^2$  at pH 8.0).<sup>36,37</sup> The electric field strength is great enough to align several layers of interfacial water molecules with a net dipole orientation toward the surface of the quartz. This leads to the comparatively strong ice-like oscillator strength

(31) The accuracy of the MALDI measurements is approximately  $\pm 10\%$ .

(32) Eisenberg, D.; Kauzmann, W. *The Structure and Properties of Water*; Oxford University Press: New York, 1969.

(33) (a) Walrafen, G. E. In *Raman and Infrared Spectral Investigations of Water Structure*; Franks, F., Ed.; Plenum: New York, 1972; Vol. 1, p 151. (b) Scherer, J. R.; Go, M. K.; Kint, S. *J. Phys. Chem.* **1974**, *78*, 1304. (c) Yalamanchili, M. R.; Atia, A. A.; Miller, J. D. *Langmuir* **1996**, *12*, 4176.

(34) Giguere, P. A. *J. Raman Spectrosc.* **1984**, *15*, 354.

(35) Note that the SFG intensity reduction upon neutral SLB formation (Figure 5a) is mainly caused by the reduction in the water-like oscillator strength rather than the ice-like oscillator strength.

(36) Iler, R. K. *The Chemistry of Silica*; Wiley: New York, 1979.

(37) Ong, S.; Zhao, X.; Eissenthal, K. B. *Chem. Phys. Lett.* **1992**, *191*, 327.

(38) Tsui, F. C.; Ojcius, D. M.; Hubbell, W. L. *Biophys. J.* **1986**, *49*, 459.

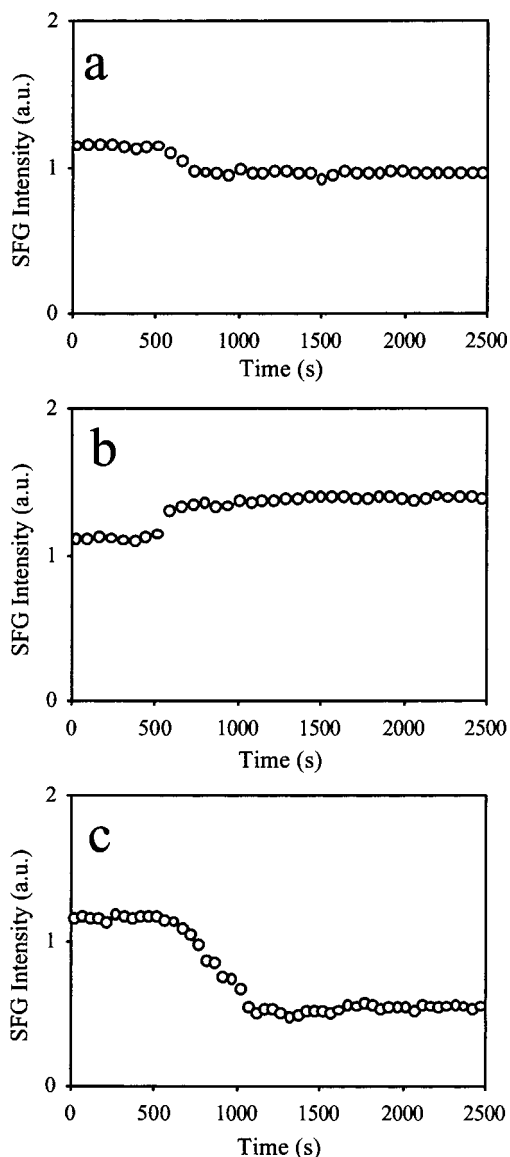


**Figure 5.** SFG signal intensity change monitored at  $3200\text{ cm}^{-1}$  by flowing solutions containing (a) neutral SUVs, (b) positively charged SUVs, and (c) negatively charged SUVs at pH 5.6.

observed at high pH (Figure 3a).<sup>18</sup> The oscillator strength of the ice-like mode attenuates as the pH is lowered; however, at very low pH (1.5), this value increases slightly again, and the net dipole moment of the water molecules is reversed.<sup>18</sup> On the other hand, the oscillator strength of the water-like peak is highest at intermediate pH (8.0). Its strength decreases at pH 12.3, where all the silanol groups are deprotonated, and also at pH 3.8 as the field strength is greatly attenuated. Under the lowest pH conditions, where all the surface silanol groups are protonated, a very small increase is again noted (Figure 3b).

#### B. Adsorption of Bilayers without a Net Charge.

The changes in the SFG spectra in terms of intensity and shape upon adsorption of an egg PC bilayer at an initially clean quartz/water interface at pH 5.6 are not as large as those from the charged membranes (Figure 2). In fact, the oscillator strength from the ice-like peak is nearly perfectly overlapped with the data from the bare surface at all pH values tested (Figure 3a). On the other hand, the oscillator strength of the water-like peak shows somewhat more substantial changes (Figure 3b). Its strength is suppressed under all pH conditions with respect to the bare surface,

but especially at pH 5.6. One possible explanation for the attenuation is that the bilayer takes up volume near the interface that is otherwise occupied by this somewhat less ordered water.<sup>39,40</sup> This idea is consistent with the notion that the first few monolayers of water above the bare liquid/solid interface mostly contribute to the  $3200\text{ cm}^{-1}$  peak, while subsequent less ordered water layers are largely responsible for the  $3400\text{ cm}^{-1}$  feature. Of course, some portion of the signal must emanate from the interface between the upper lipid leaflet and bulk water. This contribution, however, is probably quite small as the neutral bilayer leads to far less water alignment than a charged silica surface as can be shown via Langmuir trough studies.<sup>41</sup>

**C. Adsorption of Charged Bilayers.** The surface charge density on the negatively and positively charged SLBs investigated here is only about  $0.03\text{ C/m}^2$ .<sup>5,38,42</sup> While this charge density is substantially less than that of a fully deprotonated quartz surface, it appears to contribute significantly to the oscillator strength of the  $3200\text{ cm}^{-1}$  peak. From the data in Figure 3a, it can be seen that the positively charged bilayer enhanced the ice-like oscillator strength at all pH values. This may correspond to better alignment in the sandwich water region, as a positive charge on the membrane should enhance the electric field between the bilayer and the surface. By contrast, the negatively charged bilayer caused attenuation of the ice-like oscillator strength at  $3200\text{ cm}^{-1}$ , which probably emanated from disruption of the sandwich water due to a reduction in field strength. In addition to weakening the field in the sandwich layer, the presence of a negatively charged bilayer should also recruit a higher concentration of sodium ions to reside in this region than would be the case for either the neutral or positively charged bilayer. This would also lead to attenuation of the  $3200\text{ cm}^{-1}$  oscillator strength. On the other hand, the positively charged membrane should help expel sodium ions, thus causing the opposite effect.

The interface between the upper lipid leaflet and bulk water must also be considered for its contribution to the ice-like mode. The small charge on the bilayers would be expected to orient some interfacial water. The positively charged membranes should help induce alignment of water with the dipole facing away from the surface, while the negatively charged membranes should induce alignment in the opposite direction. If this were the dominant contribution, one might expect positively charged membranes to weaken the ice-like oscillator strength, since the alignment would be in the opposite direction of the sandwich water, thereby partially canceling the net dipole. On the other hand, the negatively charged membranes would have the opposite effect. Since this is not observed, it is expected that the upper leaflet's contribution is again rather small relative to the perturbation the bilayer imposes on the sandwich region.

It is clear from the data in Figure 3 that the charged SLBs have an even larger effect on the water-like peak. At pH 12.3, 10.0, and 8.0, the oscillator strength of the water-like peak from the negatively charged SLB is actually enhanced compared with the neutral SLB, while the presence of a positively charged membrane causes a net reduction in the strength. Such changes may be indicative of small differences in distance between the various SLBs and the solid substrate. Presumably, a

(39) Vogler, E. A. *Adv. Colloid Interface Sci.* **1998**, *74*, 69.

(40) Vogler, E. A. *J. Biomater. Sci., Polym. Ed.* **1999**, *10*, 1015.

(41) Kim, J.; Cremer, P. S., unreported data.

(42) Walker, R. A.; Gruetzmacher, J. A.; Richmond, G. L. *J. Am. Chem. Soc.* **1998**, *120*, 6991.

positively charged SLB would be slightly closer to the surface than one with a net negative charge. Such changes may influence the amount of water-like structure that can fill this volume. Furthermore, the presence of a small negative charge on the lower leaflet may help create more disorder in the sandwich layer, thereby increasing the  $3400\text{ cm}^{-1}$  oscillator strength at the expense of the  $3200\text{ cm}^{-1}$  mode. Considering that the  $\text{p}K_{\text{a}}$  value of the amine group in DLPS is close to 9.8,<sup>38</sup> one would expect this phenomenon to be most obvious at higher pH ( $\geq 9.8$ ) where the DLPS molecules bear a double negative charge. Indeed, the water-like value is substantially greater in the presence of the negatively charged SLB than it is from even the bare interface at pH 10.0 and 12.3.

As the pH is lowered, the oscillator strength of the water-like peak from the negatively charged SLB attenuates more rapidly than from the other systems (positive, neutral, and bare). In fact, it gives rise to the weakest signal of any of the systems investigated at pH 5.6, 3.8, and 1.5. The reason for the rapid attenuation almost certainly stems from the protonation of the carboxylic acid moiety in the DLPS containing membranes as the pH is lowered. What is striking is the fact that the water-like mode is more sensitive to this change than the ice-like mode. Again, the interface between the upper bilayer leaflet and the bulk solution is probably only a minor contribution to these effects.

#### D. Electrolyte Concentration and Kinetic Studies.

Another factor that affects interfacial water structure is the total electrolyte concentration of the bulk solution. Increasing the electrolyte concentration decreases the Debye–Hückel screening length leading to less interfacial water alignment.<sup>18,21,43,44</sup> In these experiments, the total electrolyte concentration was changed from 32 to 150 mM, corresponding to a decrease in the screening length from 2.9 to 1.4 nm.

(43) Chattoraj, D. K.; Birdi, K. S. *Adsorption and the Gibbs Surface Excess*; Plenum Press: New York, 1984.

(44) Zhao, X.; Ong, S.; Eisenthal, K. B. *Chem. Phys. Lett.* **1993**, *202*, 513.

SFG signal intensity changes as a function of time show that the rate dependence of SLB formation depends on the membrane charge (Figure 5). The relatively long time ( $\sim 800\text{ s}$ ) required to form negatively charged SLBs is presumably due to electrostatic repulsions.

#### Summary and Conclusions

We carried out investigations of water structure and dynamics at the quartz/water interface upon the formation of different SLBs by the use of vibrational sum frequency spectroscopy. This was done for numerous pH and electrolyte concentrations of the bulk aqueous solution. Generally, the oscillator strength of the water-like peak was reduced by the formation of positively charged and neutral SLBs but increased by negatively charged SLBs. On the other hand, the ice-like mode was enhanced by positively charged SLBs but reduced by those with negative charge. The SFG signal intensity changes monitored as a function of time at  $3200\text{ cm}^{-1}$  by flowing SUV solutions over initially clean quartz surfaces indicated that negatively charged SLBs form more slowly than positively charged and neutral SLBs.

**Acknowledgment.** This research was generously supported by the Robert A. Welch Foundation (Grant A-1421), the National Science Foundation (CHE-0094332), the Petroleum Research Fund (Grant 34149-G5), a Research Innovation Award from the Research Corporation of America (Grant RI0437), and startup funds from Texas A&M University. We thank Mr. Joseph Campbell and Prof. Richard M. Crooks for use of their atomic force microscope and Dr. Eric E. Simanek for the use of his light scattering apparatus.

**Supporting Information Available:** SFG spectra in the OH stretch region before and after the formation of SLBs at pH 1.5, 3.8, 5.6, 8.0, 10.0, and 12.3 with a total electrolyte concentration of 32 mM (Figure S1) and 150 mM (Figure S2); Table S1 and Table S2 for curve fit results of SFG spectra in Figure S1 and Figure S2. This material is available free of charge via the Internet at <http://pubs.acs.org>.

LA0017274